

ADENYLATE CYCLASE REGULATES ELONGATION OF MAMMALIAN PRIMARY CILIA

Young Ou¹, Yibing Ruan¹, Min Cheng¹, Joanna J. Moser¹, Jerome B. Rattner², and Frans A. van der Hoorn^{1,*}

¹ Department of Biochemistry and Molecular Biology, Faculty of Medicine, University of Calgary, 3330 Hospital Drive NW, Calgary, Alberta T2N 4N1, Canada

² Department of Cell Biology and Anatomy, Faculty of Medicine, University of Calgary, 3330 Hospital Drive NW, Calgary, Alberta T2N 4N1, Canada

Abstract

The primary cilium is a non-motile microtubule-based structure that shares many similarities with the structures of flagella and motile cilia. It is well known that the length of flagella is under stringent control, but it is not known whether this is true for primary cilia. In this study, we found that the length of primary cilia in fibroblast-like synoviocytes, either in log phase culture or in quiescent state, was confined within a range. However, when lithium was added to the culture to a final concentration of 100 mM, primary cilia of synoviocytes grew beyond this range, elongating to a length that was on average approximately 3 times the length of untreated cilia. Lithium is a drug approved for treating bipolar disorder. We dissected the molecular targets of this drug, and observed that inhibition of adenylyl cyclase III (ACIII) by specific inhibitors mimicked the effects of lithium on primary cilium elongation. Inhibition of GSK-3 β by four different inhibitors did not induce primary cilia elongation. ACIII was found in primary cilia of a variety of cell types, and lithium treatment of these cell types led to their cilium elongation. Further, we demonstrate that different cell types displayed distinct sensitivities to the lithium treatment. However, in all cases examined primary cilia elongated as a result of lithium treatment. In particular, two neuronal cell types, rat PC-12 adrenal medulla cells and human astrocytes, developed long primary cilia when lithium was used at or close to the therapeutic relevant concentration (1–2 mM). These results suggest that the length of primary cilia is controlled, at least in part, by the ACIII-cAMP signaling pathway.

Keywords

lithium; microtubules; PKC; ciliary length; synoviocytes; PC12 cells; astrocytes; bipolar disorder

*Corresponding author: Dr. Frans A. van der Hoorn, Department of Biochemistry and Molecular Biology, Faculty of Medicine, University of Calgary, 3330 Hospital Drive NW, Calgary, Alberta T2N 4N1, Canada. fvdhoorn@ucalgary.ca; Tel: 403-220-5712; Fax: 403-210-8109.

Publisher's Disclaimer: This is a PDF file of an unedited manuscript that has been accepted for publication. As a service to our customers we are providing this early version of the manuscript. The manuscript will undergo copyediting, typesetting, and review of the resulting proof before it is published in its final form. Please note that during the production process errors may be discovered which could affect the content, and all legal disclaimers that apply to the journal pertain.

INTRODUCTION

One common feature of cells found in both adult and embryonic tissues is the presence of a single, non-motile primary cilium that extends into the extracellular environment. Structurally, primary cilia share many similarities to motile cilia and flagella, each arising from a basal body and consisting of a membrane-bound ciliary axoneme. The ciliary axoneme of the primary cilium is comprised of nine doublet microtubule bundles, but lacks the central microtubule pair (termed a 9+0 structure). In addition, it lacks dynein arms and other affiliated structures seen in motile cilia and flagella (termed canonical '9 + 2' structures). Many signalling proteins, such as platelet-derived growth factor receptor alpha, polycystins and Patched, are concentrated along primary cilia [8;28;68;77;81;100]. In addition, extracellular matrix receptors are also localized to the primary cilia [48;49]. Hence, in differentiated and the interphase stage of cycling cells, primary cilia can transduce extracellular stimuli from growth factors, hormones, and odorants, and can also detect changes in osmolarity, light intensity, and fluid flow. During embryonic development, primary cilia are found to be essential for the correct functioning of vertebrate Hedgehog signalling pathway and for generation of left-right asymmetry [14;34;58;77]. Abnormal primary cilia are associated with the development of obesity, polycystic kidney diseases, cancer and other diseases (for reviews, see [3;20;67;89]).

The assembly of the primary cilium is tightly coupled to the cell cycle. The primary cilium assembles at early stages of interphase and disassembles before cell division [32;75]. After cell division, each cell inherits two centrioles. Only one of the centrioles is mature, and it is this mature centriole that develops into a basal body, giving rise to a primary cilium. The assembly process of primary cilium, or ciliogenesis, is complex and can be divided into several stages: (1) fusion of Golgi-derived membrane vesicles with the distal end of the basal body, (2) initial assembly of the 9+0 microtubule axoneme and further fusion of vesicles with more membranes to create a sheath surrounding the growing axoneme, (3) the growth of the membrane-bound axoneme to the cell surface and its fusion with the plasma membrane, and (4) further growth of the axoneme beyond the cell surface via an intraflagellar transportation system (IFT) to develop the distal part of cilium (for recent reviews see [1;69]). Once the primary cilium is formed, it is not clear what controls its final length.

In lower organisms, the length of flagella is tightly regulated. In *Chlamydomonas*, for example, if one of the two flagella in the same cell is amputated, the remaining one will transiently shrink and then regrow to the length of the amputated one, and eventually the two shortened flagella will elongate to reach the length displayed before perturbation [78]. Recent studies further showed that the two flagella of *Chlamydomonas* display <5% difference in length and are within 10% tolerance throughout the whole *Chlamydomonas* population [96]. Many factors have been identified to contribute to length control of flagella in *Chlamydomonas*, including genetic defects [39;90] and changes in intracellular and extracellular environments [6;46;88].

As for non-motile primary cilia, it has been found that the length of these cilia varies according to tissues and cell types. In liver tissue, for instance, the length of the

cholangiocyte primary cilia changes in relation to location. Thus, as the diameter of the bile duct increase, there is a corresponding increase in the length of primary cilia [33].

Studies of mouse models of renal injury have also established that renal injury results in changes in the length of renal cilia ([93;94]). In culture, cells display heterogeneous primary cilia length (short, medium, and long) ([96] and references therein). It is not known why cells display this length variation. One possible explanation is that cells are at different stages of the cell cycle. Noteworthy, Wheatley and Bowser [96] reported that cilia have a similar length (with discrepancies of less than 25% in 70% of the cases) in individual PtK1 cells that express 2 or more primary cilia. This consistency, together with the length changes seen in tissues under physiological and pathological conditions, suggests that the length of primary cilia in mammalian cells is also regulated, even though less stringent in comparison with length control of flagella in *Chlamydomonas*.

For primary cilia to function as a sensory organelle there may be a need to adjust the length of this organelle in response to extracellular environment changes. Studies of kidney cells have demonstrated that cells can regulate the length of cilia in response to environmental stimuli [74;83;93]. Loss of this length change can be a hallmark of some ciliary diseases. For instance, in a mouse model lacking Tg737, the homolog of the *Chlamydomonas* IFT88 protein, kidneys have abnormally short cilia [66], and such mice die from polycystic kidney disease. Abnormally long cilia have been associated with juvenile cystic kidney disease [87].

In the present study, we explored how the length of primary cilia is regulated. We used lithium, a drug that has been shown to alter flagellar length in *Chlamydomonas* [56;92;98], to study the possibility that lithium may also affect the mechanisms that specify the length of primary cilia in mammalian cells. Lithium has been shown to target a broad spectrum of enzymes including GSK-3 β and adenylate cyclase III (ACIII) [70;71] and hence may have distinct functions at different organisms or at different stages of a cell cycle within the same organism. In this study, we tested the effect of lithium on pre-formed or existing primary cilia in serum-starved mammalian cells such that the effect was only confined to the length change, not the formation process, of primary cilia. We found that lithium induces primary cilium elongation, and that the effect of lithium is mediated through neither GSK-3 β nor inositol-PKC, but rather through the ACIII pathway. Further, we revealed that the extent of the change in the length of primary cilia is dose dependent and cell type specific, and that two neuronal cell types reacted to the lithium treatment at a therapeutic relevant concentrations. The implications of primary cilia organization, their function and their role in neurological disorders are discussed.

MATERIALS AND METHODS

Cell culture

Human fibroblast-like synoviocytes cells and astrocytes were purchased from ScienCell Research Laboratories (CA, USA) and were cultured in cell type-specific media purchased from ScienCell. Human foreskin fibroblasts, NIH3T3 fibroblasts and PC12 cells were grown in DMEM (Gibco/BRL) supplemented with 10% fetal calf serum. For preparation of log phase cells, cells were collected by trypsin/EDTA (Gibco/BRL) treatment and re-grown

overnight on coverslips in fresh medium. For preparation of quiescent cells, log phase cells were incubated in a medium lacking serum for 48 hrs.

Radiolabeling of proteins

Log phase cells grown in 100 mm culture dishes were serum-starved for 48 hrs and then were subjected to three different treatments for 7 hrs: (1) fresh serum-free medium; (2) fresh serum-free medium containing a final concentration of 50 µg/ml or 250 µg/ml of cycloheximide; and (3) fresh serum-free medium containing a final concentration of 50 µg/ml of cycloheximide and a final concentration of 100 mM lithium chloride. One-thousand µCi of [³⁵S]cysteine was immediately added to each treatment. After 7 hrs of cultivation, cells were collected, and proteins were solubilized directly in 500 µl of SDS sample buffer. 25 µl of each sample was used and analyzed by 10% SDS-polyacrylamide gel electrophoresis. The radiolabeled proteins were visualized by autoradiography.

Drug treatment

The following drugs were used in this study: lithium chloride, valproate, myo-inositol, chelerythrine chloride, adenosine 3' monophosphate, 8-bromo-cAMP and forskolin from Sigma (St Louis, MO), GSK-3β inhibitors II, VII, and XI from EMD/Calbiochem (New Jersey, USA). Cells were serum-starved for two days prior to the drug treatment, and the concentration and duration of each drug used are described in the text.

Antibodies

Anti-acetylated tubulin antibodies and anti-β-actin antibodies were purchased from Sigma (St Louis, MO). Anti-MAP1B antibodies were from Santa Cruz Biotechnologies Inc.. Antibodies against GSK-3β, phospho (Ser-9) GSK-3β and phospho (Thr-41/Ser-37/Ser-33) β-catenin were purchased from Cell Signaling Technology (Boston, MA). Anti-ACIII antibodies were from Santa Cruz Biotechnologies Inc (California, USA). HRP-conjugated secondary antibody and Cy³-, and Alex⁴⁸⁸-labeled secondary antibodies were purchased from Jackson ImmunoResearch (West Grove, PA) and Molecular Probes (Eugene, OR), respectively.

RNA isolation and RT-PCR

RNA were isolated from two wells of monolayer cells cultivated in a 24-well plate using TRIzol (Invitrogen) under a condition recommended by the manufacturer (Invitrogen) RT-PCR was performed as described (Fitzgerald et al., 2006). Briefly, RNA was transcribed into cDNA using the M-MLV reverse kit (Invitrogen). For each sample, 100 ng of random primers was used, and a total volume of 20 µl of cDNA was generated, 2.5 µl of which were used as template for PCR in a 50 µl reaction volume. For each primer set, 30 cycles of PCR were carried out under the following conditions: a denaturing step for 30 s at 94 °C, an annealing step for 45 s at 60 °C, and an elongation step for 1.5 min at 72 °C. For PCR, the following primers were used: ACIII forward primer, ACfwd, 5'-TGC CGA GGA ACC AGG GCT TC-3'; ACIII reverse primer, ACrev, 5'-CTG ATG CAG TAG TAG CAG TCG CC-3'; housekeeping gene GAPDH forward primer, GAPDHfwd, 5'-GAC CCC TTC ATT GAC CTC AAC-3'; housekeeping gene GAPDH reverse primer, GAPDHrev, 5'-ACC ACC CTG

TTG CTG TAG CC-3'. PCR fragments were analyzed in a 1.2% agarose gel, and sequence analysis of the cDNA fragments was determined at the University of Calgary Core DNA Services.

Western blot

Western blot analysis was carried out essentially as described previously [22]. In short, proteins were boiled in loading buffer, separated on 10% acrylamide SDS-PAGE gels, electrophoretically transferred onto a polyvinylidene fluoride membrane (Amersham Biosciences), blocked overnight at 4 °C in blocking buffer (54 mM Tris, pH 7.5, 150 mM NaCl, 0.05% Nonidet P-40, 0.05% Tween 20, 5% dry nonfat milk), and analyzed using primary antibodies followed by HRP-conjugated secondary antibody. Prestained Protein Ladder SM0671 (Fermentas) was used as a size marker. LumiGLO substrate (Kirkegaard & Perry Laboratories, Inc.) was used to develop the blot. The luminescent image was captured using a 3000 Versa-Doc Imaging System (Bio-Rad).

Immunofluorescence microscopy and length measurement of primary cilia

Indirect immunofluorescence microscopy (IIF) was performed as described previously [62;63]. Briefly, cells were fixed in cold methanol and stained with primary and secondary antibodies at a concentration recommended by the companies. Images were obtained by using the Leica PL APO 100×/1.40-0.7 oil objective lens and a 1.0× magnification tube attached to a CCD camera. The length of primary cilia was measured as described by Tam et al., (2007) using NIH IMAGEJ software, by tracing the midline of primary cilia, with parameters (the ratio of fluorescent image pixel dimension vs. actual size of an object in micrometer) predetermined using stage objective micrometer (Nikon).

Scanning and transmission electron microscopy

For scanning electron microscopy, cells were fixed with 2% glutaraldehyde in Millong's phosphate buffer and then with 1% osmium tetroxide in Na-cacodylate buffer, dehydrated in ethanol and critical-point dried. After coating with a layer of colloidal gold, the samples were examined using a Philips XL30 ESEM scanning electron microscope. Transmission electron microscopy was performed as described previously ([64]). Briefly, cells were fixed in 2% glutaraldehyde and 1% osmium tetroxide, respectively. Cells were then counter-stained with 2% uranyl acetate, dehydrated in ethanol, embedded in Epon resin, and sectioned. The samples were examined using a Hitachi-7650 microscope.

Statistic analysis

Data are presented as the mean value or mean \pm s.d. (standard deviation) of at least three independent experiments. Student's *t*-test was used to determine *P* value. *P* values less than 0.05 are considered to be significant.

RESULTS

The length of primary cilia in fibroblast-like synoviocytes in log phase and quiescent state is similar

To study the effects of lithium on cells, we first analyzed primary cilia in cultured human synoviocytes. The synovial membrane contains an intimal lining of two or three layers of macrophage-like and fibroblast-like cells embedded in a dense extracellular matrix [25]. The fibroblast-like synoviocytes (FLS) are the predominant cells that, in response to extracellular stimuli, secrete collagen, fibronectin, hyaluronan, and other proteoglycans into the interstitium and joint cavity. These cells also have endocrine and sensory function and participate in the development of rheumatoid arthritis [36]. Electron microscopic images verify that each FLS contains a single primary cilium that projects into the luminal surface of the synovial membrane from the bottom of a deep invagination of the cell membrane [25;82;86;99]. FLS can be isolated and maintained in culture for up to 15 passages during which time they continue to express primary cilia.

We first established the length of primary cilia in log phase FLS primary cells by staining cells with antibodies to acetylated tubulin and measuring their length in immunofluorescence images. Anti-acetylated tubulin antibody has been widely used to detect primary cilia by IIF. In log phase cultures, 14.7% (44/300) of FLS cells express primary cilia with lengths of 1.52 μm to 9.09 μm (average length = 4.50 μm , standard deviation (s.d.) = 1.35, n=44). Thus, FLS cells also express short, medium, and long primary cilia characteristic of PtK1 cells [96]. This heterogeneity is not surprising since cells are at distinct stages of the cell cycle. To address this we incubated cells in a serum-deprived culture medium for 48 hrs. In the resulting quiescent state, 93% (279/300) of FLS cells were found to display primary cilia with an average length of 4.40 μm (ranging from 1.83 μm to 6.91 μm , standard deviation of 0.77, n=279). Although quiescent FLS cells also display heterogeneity in primary cilium length, the variation is less extensive. The average primary cilium length was the same between cells in log phase and quiescent cells.

To further examine cell to cell variation, we measured ciliar length in those cells that expressed two primary cilia. Supplemental Table 1 shows the results for 32 of these cells. Analysis indicates that the two cilia on the same cell have no significant difference in length ($p < 0.05$). This result suggests that the length of primary cilia, like those of flagella, is also under stringent control.

Lithium induces primary cilium elongation in FLS cells

Lithium had been shown to affect the length of flagella in *Chlamydomonas* [56;92;98]. In this study, we analyzed the effect of lithium on primary cilium length in FLS cells. To exclude the multiple effects that lithium may have on diverse cellular activities, we made use of serum starvation conditions established above to investigate the length changes of pre-formed or existing primary cilia in serum-starved FLS primary cells. We first carried out a series of pilot studies and found that lithium indeed induces a change in cilium length in FLS cells (Fig. 1, compare control and lithium) where primary cilia elongate well beyond the length range measured from untreated cells (see above). We next determined the

relationship between concentration and duration of exposure to the drug and cilium elongation. FLS cells were serum-starved for 48 hrs, treated for 12 hrs with lithium at various concentrations, and stained using anti-acetylated tubulin antibody. The results shown in Fig. 2A indicate that cells displayed elongated cilia at concentrations as low as 5 mM of lithium treatment ($p < 0.05$ in comparison with 0 mM; $n = 150$), and cilium length reached a maximum at 100 mM of lithium, the highest concentration tested. When cells were treated with 100 mM lithium chloride, cells started to show increased cilium length at 60 minutes post treatment ($p < 0.05$ in comparison with 0 hr; $n = 150$), and the majority of cilia showed significant elongation at 12–21 hours. Thereafter, the length of the primary cilia population started to decline (Fig. 2B). It should be noted that, although primary cilia were longest at the 21 hour time point, cytotoxic effects (morphology change) were also evident (data not shown). Primary cilia elongation was not observed in cells treated with equal molar concentration of NaCl (data not shown), suggesting that primary cilium elongation is not caused by monovalent cation and is specific for lithium.

Using the treatment condition of 100 mM lithium for 12 hours, we measured the length of primary cilia in serum-starved FLS cultures before and after treatment. As before, FLS cells were stained with anti-acetylated tubulin antibody. We found that after lithium treatment the length of primary cilia had reached an average length of 12.49 μm with a standard deviation of 3.85 ($n = 40$), and some cilia reached a maximal length of 17.22 μm . On average the treated cell population had cilia lengths that were on average 3 times those found in untreated cultures. Thus, lithium induces the elongation of pre-formed or existing primary cilium.

To extend this observation, we measured the possible effect of lithium on the % of cells with a primary cilium. In log phase cultures, 15.3% (46/300) of lithium-treated cells displayed primary cilia in comparison with 14.7% (44/300) in untreated cells (see above). This result suggests that lithium does not promote cilia formation. When serum-starved culture was treated by lithium, 87.7% (263/300) of lithium treated cells display primary cilia in comparison with 93% (279/300) of untreated cells. Thus, it appears that, in all cases (log phase or serum-starved), lithium affects preformed or existing cilia, causing them to elongate.

Lithium induced primary cilium elongation does not require protein synthesis

Serum starvation causes cells to exit the cell cycle, while maintaining a basal level of metabolism. Thus, it is possible that lithium treatment of serum-starved FLS cells could lead to elevated protein synthesis and this in turn could impact cilium elongation. To investigate this possibility, we first treated serum-deprived FLS cells with the protein synthesis inhibitor cycloheximide at a concentration of either 50 $\mu\text{g/ml}$ or 250 $\mu\text{g/ml}$ for 3 hrs and then measured primary cilium lengths as before. Under these conditions, protein synthesis was completely inhibited (see supplemental Fig. S1). Cilia treated with cycloheximide exhibited the same length as those found in untreated cultures (Fig. 2C, compare CTL, A and C). Further, when cultures were grown in the presence of cycloheximide for 3 hours and then co-treated with cycloheximide and lithium for 7 hrs, cilium elongation was observed and the average length of cilia was similar to that observed in lithium-treated cultures in the absence

of cycloheximide (Fig. 2C, compare Li, B and D). Co-treatment of cells with cycloheximide and lithium did not restore protein synthesis (supplemental Fig. S1). These results suggest that primary cilium elongation by lithium does not require *de novo* protein synthesis and post-translational modification of protein(s) is possibly responsible for the elongation process.

The structure of primary cilia is not altered by lithium treatment

To determine if lithium causes structural changes in the primary cilium in concert with ciliary elongation, we prepared lithium-treated cultures for scanning (SEM) and transmission (TEM) electron microscopy. In SEM micrographs taken from untreated FLS cultures, primary cilia could be seen extending outward from an invagination or pit in the plasma membrane (Fig. 3A, left image). Similarly, the elongated primary cilia of lithium treated FLS cultures protruded from invaginations (Fig. 3A, right image). Cilia from both treated and untreated cultures displayed similar diameters. Blebs seen on these cilia may represent IFT particles (Fig. 3A, arrowheads). We also used SEM to measure the length of FLS primary cilia. Measurements of untreated cilia and treated cilia indicated that the lengths of the protruded portion were $1.34 \pm 0.52 \mu\text{m}$ (mean + standard deviation; $n=50$) and $6.48 \pm 1.71 \mu\text{m}$ ($n=17$), respectively. This result clearly confirmed that the primary cilia grew significantly (more than 3 times in length) after lithium treatment, consistent with the estimates obtained from measuring fluorescence images.

TEM micrographs from both untreated (Fig. 3B, CTL) and treated (Fig. 3B, T1–3) cultured FLS cells revealed that primary cilia emanating from the basal body were positioned some distance below the plasma membrane. As a result, in agreement with previous TEM images [25;82;86;99], a portion of the axoneme, in both conditions, is positioned within a membrane invagination that is continuous with the plasma membrane, and the invagination is lined with Golgi complexes (Fig. 3B, CTL, arrowheads, and data not shown). Cross-sectional profiles of the axoneme of primary cilia from both untreated and lithium-treated cells displayed the typical 9+0 microtubule pattern (Fig. 3B, T3). Due to bending of the cilium one often observes both microtubule doublets as well as an oblique profile. We also found that the microtubule doublets extended to the tip of the cilium (Fig. 3B, T2, arrows), indicating that the cilium architecture is maintained throughout the cilium shaft in the presence of lithium.

Inhibition of GSK-3 β does not trigger primary cilia elongation

Lithium has been shown to inhibit a number of enzymes, which include GSK-3 β , IMPase and IPPase, and adenylate cyclase III [72]. GSK-3 is a serine/threonine kinase that plays a central role in regulation of glycogen synthesis and in modulating many molecular signaling cascades, including the Wnt pathway, insulin-AKT pathway and RasGTP-RSK pathway. GSK-3 β can phosphorylate approximately 50 downstream target proteins, among which are microtubule-associated protein MAP1B and β -catenin [23]. In particular, GSK-3 β phosphorylates MAPs, participating in regulation of microtubule stability.

It was shown that inhibition of GSK-3 β by lithium affects the formation and possibly the length of flagella in *Chlamydomonas* [98]. Although flagella in *Chlamydomonas* and

mammalian primary cilia share some structural similarities they are functionally very different (motility and mating vs. sensing). Here we sought to investigate if the observed lithium-mediated elongation of primary cilia in FLS cells is dependent on GSK-3 β or other proteins.

First we sought to determine any direct effects of lithium on GSK-3 β . Lithium has a dual inhibitory function on GSK-3 β kinase activity: first, it acts as a noncompetitive inhibitor of magnesium and directly inhibits GSK-3 β activity with a K_i of 1–3 mM. Second, lithium can inhibit GSK-3 β activity by increasing the phosphorylation of the inhibitory serine (Ser-9) of GSK-3 β [16]. We studied the effect of lithium on phosphorylation of GSK-3 β Ser-9 by western blot using an anti-phospho-epitope (Ser-9)-specific GSK-3 β antibody. The result (Fig. 4A) illustrates that lithium treatment causes phosphorylation of GSK-3 β Ser-9 in FLS cells, as expected. Second, we tested effects of lithium on two GSK-3 β substrates MAP1B and β -catenin. GSK-3 β is constitutively active in cells under basal conditions, phosphorylates MAP1B, promotes MAP1B binding to microtubules and causes stabilization of microtubules [12]. The effect of GSK-3 β on MAP1B was studied by observing the pattern of MAP1B association with microtubules in FLS primary cells. Our IIF results shown in Supplemental Fig. S2 demonstrate that MAP1B binds to microtubules under conditions of serum starvation. After lithium treatment MAP1B disassociates from microtubules and remains cytosolic. Thus, inhibition of GSK-3 β activity by lithium induces the release of MAP1B from the microtubules. Given that microtubule-binding of MAP1B leads to microtubule stabilization, microtubule disassociation of MAP1B after lithium treatment could possibly decrease microtubule stability raising the question as to how lithium inhibition of GSK-3 β activity could promote growth of the primary cilium. Finally, we studied the phosphorylation state of β -catenin: it has been shown that β -catenin is a downstream target of GSK-3 β that is, in particular, regulated by Wnt signaling pathway. Western blot analysis of the phosphorylation state of β -catenin is a measure of GSK-3 β activity [12]. Our results using an antibody that recognizes phosphorylated (Thr-41/Ser-37/Ser-33) β -catenin (Fig. 4B) illustrate that lithium treatment of FLS cells leads to loss of phospho-epitopes of β -catenin. Taken together, the above results confirmed that lithium treatment affects GSK-3 β activity and regulates GSK-3 β downstream substrates in serum-starved FLS cells.

To investigate then a possible role for GSK-3 β in primary cilium elongation, we made use of inhibitors specific to this protein kinase to determine if GSK-3 β inhibition could promote cilia elongation. We tested four different inhibitors of GSK-3 β : valproate [11;26], GSK-3 β inhibitor II (IC_{50} = 390 nM; [38;55;84]), GSK-3 β inhibitor VII (IC_{50} = 500 nM; [13]), and GSK-3 β inhibitor XI (IC_{50} = 25 nM; [59]). The effectiveness of each of these GSK-3 β inhibitors was verified by observation of changes in FLS cells morphology, by IIF using anti-MAP1B antibody, and/or by western blot using anti-phospho- β -catenin antibody (Fig. 4B, and data not shown).

Serum-starved FLS cells were cultured for 12 hrs in the presence of each of these inhibitors at various concentrations and assayed for cilium lengths. Valproate inhibits GSK-3 β activity at 1 mM concentration [11], but we could not detect any changes of primary cilium lengths using this inhibitor at concentrations from 1.56 mM up to 12.5 mM (Fig. 5A). Similarly, we

titrated GSK-3 β inhibitors II and VII from 0.625 μ M to 10 μ M, and found that neither of these two inhibitors at these concentrations tested could cause primary cilium elongation (Fig. 5B for GSK-3 inhibitor VII; GSK-3 inhibitor II, data not shown). As well, we titrated GSK-3 β inhibitors XI from 25 nM to 250 nM, without seeing any effects on the length of pre-formed primary cilia (data not shown). We conclude that although lithium affects GSK-3 β activity, its inhibition is not the mechanism that underlies the observed primary cilium elongation in mammalian cells.

Inhibition of PKC activity does not induce primary cilia elongation

PKC has been found to be implicated in the formation of cilia in mammalian cells [21;85]. Lithium inhibits both IMPase and IPPase, two enzymes required for converting inositol-1,2,5-triphosphate (IP3) to myo-inositol [27;35], causing a reduction in myo-inositol [2] and as a consequence attenuation of PKC signaling pathway [29;42]. This suggested that the phosphoinositol-PKC pathway may be involved in primary cilium elongation observed after lithium treatment.

We treated serum-starved synoviocytes with chelerythrine chloride, a potent and specific inhibitor of PKC [19;30], which can block translocation of PKC from cytosol to the membrane [10]. In addition, chelerythrine chloride reduces anterograde and retrograde axonal transport in cultured isolated mouse dorsal root ganglion cells [31]. Serum-starved FLS cells were subjected to treatment by the inhibitor at 10 μ M concentration for various times. At this concentration chelerythrine chloride was confirmed to effectively inhibit PKC activity (data not shown). Our results (Fig. 5C) demonstrate that inhibition of PKC by chelerythrine chloride did not induce primary cilia elongation, but instead caused shortening of primary cilia.

Adenylate cyclase III is localized to primary cilia in synoviocytes and its inhibition induces primary cilia elongation

Numerous studies have indicated that lithium affects ACIII activity and impairs cAMP production (e.g. [17;18;44;54;57;76]). There are three classes of adenylate cyclases identified in organisms from prokaryotes to mammals, among which adenylate cyclase class III (ACIII) which is the only class found in mammalian cells (for review see [41]). ACIII can be membrane-associated, or exist in a soluble form. One major target of cAMP is PKA. Lithium can thus modulate PKA-mediated protein phosphorylation, in particular phosphorylation of cytoskeletal proteins (e.g. [9;52;53]).

First we show here that ACIII is a component of the primary cilia of untreated and lithium-treated FLS synoviocytes (Fig. 6). Next we treated FLS cells for 60 hrs with two ACIII P-site inhibitors: first, we titrated adenosine 3' monophosphate (3'-AMP) and found that at 5 mM this inhibitor resulted in elongation of primary cilia, on average, to 7.95 μ m (n = 33) from 4.28 μ m for untreated cells (n = 23) ($p < 0.05$) (Fig. 7A). Similar results were found when FLS cells were treated with this inhibitor for 36 hrs (6.27 μ m for treated cells (n = 43) vs. 4.19 μ m for untreated cells (n = 40)). We next titrated dideoxyadenosine triphosphates and found that this inhibitor caused primary cilium elongation at 500 μ M (4.32 μ m for untreated cells vs. 5.89 μ m for treated cells) ($p < 0.05$) (Fig. 7B). These results show that

ACIII inhibition can result in primary cilia elongation, but that these two inhibitors did not cause elongation to the same extent possibly due to distinct specificities of these two inhibitors for the ACIII isoforms [44]. Also, these two inhibitors did not induce primary cilium elongation to the extent observed for lithium, suggesting that these two inhibitors may affect only part of the ACIII pool in comparison with possible inhibition of all ACIII isoforms by lithium.

We next tested the effect of two ACIII activators, forskolin and 8-bromo-cAMP, on the length of primary cilia. Interestingly, these two activators were unable on their own to induce a significant change in primary cilia length (Fig. 7C, forskolin; Fig. 7D, 8-bromo-cAMP). However, when these two activators were used prior to lithium treatment, the combined treatment induced moderate primary cilium elongation, suggesting that stimulation of ACIII activity interfered with lithium inhibition (Fig. 7C, compare Li and 'F+L'; Fig. 7D, compare Li and 'BcAMP+Li'). Together, these results indicate that inhibition of ACIII impacts primary cilia length, and this may explain in part the effect of lithium on primary cilium elongation.

Lithium causes primary cilium elongation in a variety of cell types

To extend our findings, we screened a number of primary cilia-expressing cells types to determine if ACIII is a component of primary cilia and if lithium induced changes in cilium length in a cell type-independent manner. We found that primary cilia from human foreskin fibroblasts (Supplemental Fig. S3, A, HFF), NIH 3T3 fibroblasts (Supplemental Fig. S3, A, NIH 3T3), rat PC12 cells (derived from a pheochromocytoma of the rat adrenal medulla) (Supplemental Fig. S3, B) and human astrocytes (data not shown) all contain ACIII. Treatment of two fibroblast cell types (human foreskin fibroblasts and mouse NIH 3T3 fibroblasts) with lithium resulted in primary cilium elongation as seen for FLS cells (Supplemental Fig. S3, A).

However, the two neuronal cell types appeared more sensitive to lithium treatment. Primary cilium elongation in PC12 cells was already seen at 2 mM lithium treatment ($p < 0.05$), reaching a maximum at 5 mM lithium ($p < 0.01$) (Fig. 8A). At higher concentration primary cilium elongation was not detected (Fig. 8A). Astrocytes, at 1 mM lithium, a concentration used in bipolar disorder therapy, showed a significant increase in primary cilium length in comparison with untreated control ($p < 0.05$). Primary cilia in astrocytes continued to elongate in a lithium dose-dependent manner (Fig. 8B). We conclude that ACIII is present in the primary cilia of all cell types examined and that lithium treatment induces changes in cilium length in all cells examined. Further, the sensitivity of primary cilia elongation by lithium is cell type-specific, with neuronal cells (PC-12 cells and astrocytes) showing highest sensitivity.

DISCUSSION

Lithium has been shown to have multiple targets and cause a multitude of changes in cell morphology, behavior, functionality, and fate as well as embryo development. In sea urchin species, for instance, lithium is a vegetalizing agent, and treatment of ciliated embryos with lithium has been shown to cause an expansion of vegetal cell fates at the expense of animal

cell fates ([97] and references therein). In *Chlamydomonas*, lithium treatment cause flagellar elongation [56;92;98]. In this study, we tested the effects of lithium in mammalian cells on primary cilium length regulation. To eliminate the multiple effects of lithium, we used quiescent cells induced by serum starvation. In the quiescent state cells have a basal level of transcriptional and translational activities, but have well-formed primary cilia. Thus, using quiescent cells as model, the activity of lithium, if any, on cilia is on their shortening or elongation, not formation.

We demonstrate in this study is that, under normal circumstances, primary cilia stop growing when reaching a particular length and that this process can be disturbed by lithium treatment. Lithium induces elongation of primary cilia and this effect is mimicked by inhibition of ACIII, a well-recognized lithium target and a component of primary cilia. Further, we show that lithium treatment affects primary cilia in a variety of cell types, among which are two neuronal cell types (rat PC-12 adrenal medulla cells and human astrocytes) that appear to be more sensitive to lithium treatment than fibroblasts. In addition, we also found that inhibition of PKC results in cilium regression, suggesting that multiple signaling pathways are implicated in primary cilium length control.

Control of the size of primary cilia

Primary cilia from mammalian cell cultures, either in log phase or quiescent, are heterogeneous in size, suggesting that the length of primary cilia, unlike that of flagella in the unicellular alga *Chlamydomonas*, may not be under tight control. However, several arguments do not support this possibility. First, cell populations from log phase cultures are heterogeneous in terms of cell cycle stages. Since primary cilium formation is tightly coupled to the cell cycle, cells at the early cell cycle stage may display short cilia while cells at later stage will have formed longer ones. Second, even in the quiescent state, different cells may have distinct intracellular environments, which may cause variations in primary cilia length. One way to study the control of the length of primary cilia is to use those cells that have two or more cilia. In our own studies, we confirmed that two primary cilia on the same cell have the same length (Supplemental Table 1). Third, we show that primary cilia from heterogeneous cell populations (log phase or quiescent) have their length regulated within a confined range. When FLS cells are kept in a quiescent state for 3 weeks, primary cilia do not elongate. However, when these cells are treated with lithium, primary cilia can grow to a length comparable to the one seen in treated log phase cells (Ou and van der Hoorn, unpublished). These results demonstrate that the reason for primary cilia to stop growing is not due to the absence of material to support further growth, suggesting that there must be a mechanism that controls the length of primary cilia. Finally, a number of studies have found that a change in the length of primary cilia occurs in tissues and cultured cells under physiological and pathological conditions [33;66;74;83;87;93;93;94]. In this study, we provide evidence that inhibition of ACIII and PKC leads to elongation and shrinking of primary cilia, respectively. These observations suggest that it is the balance of different signaling pathways that defines the length of primary cilia. To our knowledge, this is the first demonstration that the length of primary cilia is controlled via mechanisms involved in signal transduction.

GSK-3 β , flagellar elongation and primary cilia formation

GSK-3 β has been reported to be involved in the regulation of formation and elongation of flagella in *Chlamydomonas reinhardtii* [98]. However, the data indicated that lithium marginally inhibits GSK-3 activity in total protein extracts (membrane plus matrix fraction) but causes a two-fold increase in the active form of GSK-3 β in the flagella. In mammalian cells, it has been found that inhibition of GSK3 activity by the GSK-3 β specific inhibitor VIII alone does not alter the length of primary cilia [98]. It is the combined inactivation of the von Hippel-Lindau protein (pVHL) and GSK-3 β that leads to the loss of cilia. In this study, we confirmed that lithium affects GSK-3 β activity. However, we used four different GSK-3 β inhibitors, and found that under conditions which greatly exceeded their IC50 none of the inhibitors caused preformed primary cilia to elongate in mammalian cells.

It is possible that distinct pools of GSK3 exist in cells. Emerging evidence suggests that growth factors and Wnt proteins may regulate distinct pools of GSKs that phosphorylate distinct set of downstream targets ([12] and references therein). For instance, Wnt3a regulates GSK3-mediated phosphorylation of β -catenin, not collapsing response mediator protein (CRMP), while IGF1 regulates GSK3-mediated phosphorylation of CRMP, not β -catenin. Thus, based on data from our lab and those of others, we conclude that lithium inhibition of the pools of GSK-3 β affected by the specific inhibitors tested is unlikely the mechanism that underlies the observed primary cilium elongation.

ACIII, cAMP signaling, and primary cilia

In *Chlamydomonas reinhardtii*, ACIII activity is detected in the gamete's cell body and flagella, with the highest specific activity displayed in flagellar membrane fractions [65]. This membrane form of ACIII is important for generating a high level of cAMP, a signal that initiates the cells for fusion to form a zygote. During the mating process, the elongation of the A microtubule in the flagella can be seen [65]. Yet, it is not known whether this elongation is related to the elevated level of cAMP or due to other coincidentally activated signaling pathways. Lithium has been found to affect flagellar length in *Chlamydomonas* [56;92;98]. Since lithium targets many proteins including ACIII, it would be interesting to test if the elongation of flagella induced by lithium is caused by the interference of ACIII (and cAMP) in *Chlamydomonas*.

In this study, we found that ACIII is expressed at primary cilia of all cell types examined, including in human fibroblast-like synoviocytes, human foreskin fibroblasts, mouse NIH 3T3 fibroblasts, rat PC12 adrenal medulla cells and human astrocytes and that inhibition of ACIII causes elongation of primary cilia. A specific isoform of ACIII was found enriched at the cilia of olfactory sensory neurons [4]. These cilia, like primary cilia, are a non-motile structure that project from the apical dendrites of the neurons into the nasal lumen and are accessible to airborne-odorants. In addition to olfactory sensory neurons, ACIII was also found in many regions of adult mouse brain, where it is enriched in primary cilia of neurons, choroid plexus cells, and astrocytes [5;7]. The functional significance of ACIII localization in the brain is not clear. It is possible that, as in the cilia of olfactory sensory neurons, ACIII and cAMP signaling contribute to changes in membrane potential and altering neuronal firing rate [7]. Outside of the nervous system, ACIII (isoforms V and VI) was found at

primary cilia of liver cholangiocytes [47] and a renal epithelial cell type [73]. Cholangiocyte cilia detect changes in luminal bile flow and ACIII functions to transmit luminal fluid flow stimuli into intracellular calcium and cAMP signaling. ACIII in the renal epithelial cells is associated with a type-2 vasopressin receptor, which when activated, initiates a functional cAMP-PKA signaling pathway that targets channel activity of primary cilia. Taken together, these data suggest that ACIII-cAMP signaling pathway is integral to primary cilia's sensing function.

Activation of ACIII produces cAMP. cAMP modulates a number of downstream effectors, which include PKA, Epac (exchange protein activated by cAMP or cAMP-regulated GTP exchange factors) and cyclic nucleotide-gated cation channels. In agreement with these central roles we observed that siRNA-mediated knockdown of ACIII was lethal to cells, preventing observation of its effects on primary cilia length (data not shown).

PKC and primary cilia

PKC belongs to a family of serine/threonine protein kinases with more than 10 isoforms. Whether this family of proteins regulates some steps of ciliogenesis is controversial. On one hand, one of the PKC isoforms, atypical PKC- ζ (aPKC ζ), forms a complex with cell polarity proteins Par3 and Par6, and this complex is found at primary cilia [21]. Depletion by siRNA- or shRNA-based techniques of par3 or of a Par3-interacting partner 14-3-3 η [37], abolishes primary cilium formation in MDCK cells [21;85]. aPKC ζ also interacts with the von Hippel-Lindau tumour suppressor protein (pVHL) in HEK293T cells [61] and co-localizes with pVHL at primary cilia of MDCK cells [80]. pVHL is required for stabilization of primary cilia [91]. On the other hand, transgenic mice with a homozygous aPKC ζ null mutation fail to confirm any obvious ciliary function that this protein might play [40].

Lithium does not directly inhibit PKC, but lithium inhibits activities of both IMPase and IPPase [27;35], which initiates a cascade of secondary changes in PKC signaling pathway. Using a specific inhibitor of PKC we did not observe a lengthening of cilia, but instead cilium regression. At present, it is not clear how PKC regulates the decrease in primary cilium length.

How does a cell regulate the length of its primary cilium?

Primary cilia start to form once cells enter interphase. Forcing cells to enter the G0 state by serum starvation, results in a large percentage of cells expressing primary cilia. Serum deprivation is accompanied by an increase in intracellular cAMP concentration [50;60]. Together with our observation that inhibition of ACIII causes ciliar elongation this raises two questions: 1) is formation of primary cilium associated with elevation of the cAMP concentration and 2) is the elevated cAMP concentration responsible for halting of primary cilium elongation?

Based on our observations and those of others, we propose a model of primary cilium length control (Fig. 11). Primary cilia form and grow when cells enter a quiescent state (differentiation, serum deprivation) or enter the early stage of interphase. G α s proteins are activated (and/or G $\beta\gamma$ proteins inactivated) which in turn activates ACIII, producing increased amounts of cAMP. cAMP modulates multiple downstream effectors (PKA, cAMP-reactive

GTP exchange protein), resulting in a rise in intracellular calcium concentration. Collectively, these factors act on primary cilia, and when primary cilia reach a particular length, they stop growing (Fig. 9A). In this state, the machinery involved in primary cilia growth (such as IFT) remains intact. Since a higher calcium concentration is required for continuous maintenance of the cells in proliferation arrest or the differentiated state (see review [79]), this higher calcium concentration may also function to maintain primary cilia at a particular length. Addition of lithium to these cells affects ACIII and cAMP signalling (Fig. 9B). As well, addition of lithium attenuates intracellular calcium mobilization [95]. Reduction of intracellular cAMP and/or calcium levels reverses the activities of these secondary messengers on a number of downstream effectors and hence releases the inhibitory control of those effectors on primary cilia growth machinery, leading to primary cilia elongation.

The dynamics and stability of primary cilia can be affected by signaling pathways that impact microtubule dynamics and instability. One such pathway is indeed ACIII-cAMP. Lithium modulates PKA-mediated protein phosphorylation. Lowered cAMP production in lithium treated cells may reverse PKA phosphorylation of cytoskeleton proteins and promote microtubule assembly and stabilization. In preliminary experiments we used siRNA to knock down PKA expression in FLS cells and human foreskin fibroblasts. Although we observed a greater than 50% decrease in PKA mRNA levels, the stability of the catalytic subunit of PKA prevented the efficient reduction in the amount of PKA protein (not shown). Thus, it remains to be determined if PKA is involved in the regulation of primary cilium elongation after lithium treatment.

Alternatively, ACIII may affect microtubule dynamics and stability through its upstream regulator G proteins. It has been found that a subset of G proteins interact directly with cytoskeletal components to modify microtubule-dependent cellular processes [15]. In particular, the same domains ($\alpha 2$ - $\beta 5$ and $\alpha 3$ - $\beta 5$) on $G\alpha$ stimulatory subunit ($G\alpha_s$) that bind to tubulins also interact with ACIII and $G\beta\gamma$ (Layden et al., 2008). $G\alpha_s$ destabilizes microtubules by activating the GTPase activity of tubulin, while $G\beta\gamma$ subunits stimulates microtubule stability by promoting microtubule polymerization. Thus, it is possible that lithium binding to ACIII mediates a conformational change in ACIII, which alters cAMP production and also leads to a higher affinity of ACIII binding to $G\alpha_s$. The formation of the ACIII- $G\alpha_s$ complex releases $G\beta\gamma$ from heterotrimeric G proteins and reduces $G\alpha_s$ -mediated GTPase activity, thereby increasing the stability of microtubules and cause microtubules (primary cilia) to elongate.

Impact of lithium on primary cilia length and its relevance to human diseases

Lithium is a drug used for treatment of bipolar disorder. One observation made in patients with bipolar disorder is cAMP signaling abnormalities. Post-mortem brain tissues from patients reveal, when stimulated by agonists, not only increased levels of binding of GTP to $G\alpha_s$ but also increased amounts of $G\alpha_s$ in comparison with age- and sex-matched normal controls (e. g. [24;43;101;102]). Lithium administration attenuates the fluctuation of cAMP levels in the central nerve system [44;45;51]. In this study, we found that inhibition of ACIII by both lithium and specific inhibitors caused primary cilia elongation. In addition, we

found that neuronal cells (astrocytes and PC12 cells) extend primary cilia when lithium is used at or close to the therapeutic dose. These findings raise the possibility that bipolar disorder is associated with abnormal primary cilia, structurally and/or functionally. In future studies, it will be important to determine if lithium affects primary cilia in animal models and if bipolar disorder can be added to the growing list of human ciliopathies.

Supplementary Material

Refer to Web version on PubMed Central for supplementary material.

Acknowledgments

We thank Eileen Rattner for excellent technical support in tissue culture and Dr. Derrick Rancourt for providing HFF cells. This project is supported by grants from the Canadian Institutes of Health Research and Alberta Cancer Board to FAvdH.

Reference List

1. Alieva IB, Vorobjev IA. Vertebrate primary cilia: a sensory part of centrosomal complex in tissue cells, but a “sleeping beauty” in cultured cells? *Cell Biol Int*. 2004; 28:139–150. [PubMed: 14984760]
2. Allison JH, Stewart MA. Reduced brain inositol in lithium-treated rats. *Nat New Biol*. 1971; 233:267–268. [PubMed: 5288124]
3. Badano JL, Mitsuma N, Beales PL, Katsanis N. The ciliopathies: an emerging class of human genetic disorders. *Annu Rev Genomics Hum Genet*. 2006; 7:125–148. [PubMed: 16722803]
4. Bakalyar HA, Reed RR. Identification of a specialized adenylyl cyclase that may mediate odorant detection. *Science*. 1990; 250:1403–1406. [PubMed: 2255909]
5. Berbari NF, Bishop GA, Askwith CC, Lewis JS, Mykytyn K. Hippocampal neurons possess primary cilia in culture. *J Neurosci Res*. 2007; 85:1095–1100. [PubMed: 17304575]
6. Berman SA, Wilson NF, Haas NA, Lefebvre PA. A novel MAP kinase regulates flagellar length in *Chlamydomonas*. *Curr Biol*. 2003; 13:1145–1149. [PubMed: 12842015]
7. Bishop GA, Berbari NF, Lewis J, Mykytyn K. Type III adenylyl cyclase localizes to primary cilia throughout the adult mouse brain. *J Comp Neurol*. 2007; 505:562–571. [PubMed: 17924533]
8. Brailov I, Bancila M, Brisorgueil MJ, Miquel MC, Hamon M, Verge D. Localization of 5-HT(6) receptors at the plasma membrane of neuronal cilia in the rat brain. *Brain Res*. 2000; 872:271–275. [PubMed: 10924708]
9. Casebolt TL, Jope RS. Effects of chronic lithium treatment on protein kinase C and cyclic AMP-dependent protein phosphorylation. *Biol Psychiatry*. 1991; 29:233–243. [PubMed: 2015330]
10. Chao MD, Chen IS, Cheng JT. Inhibition of protein kinase C translocation from cytosol to membrane by chelerythrine. *Planta Med*. 1998; 64:662–663. [PubMed: 9810275]
11. Chen G, Huang LD, Jiang YM, Manji HK. The mood-stabilizing agent valproate inhibits the activity of glycogen synthase kinase-3. *J Neurochem*. 1999; 72:1327–1330. [PubMed: 10037507]
12. Cole AR, Sutherland C. Measuring GSK3 expression and activity in cells. *Methods Mol Biol*. 2008; 468:45–65. [PubMed: 19099245]
13. Conde S, Perez DI, Martinez A, Perez C, Moreno FJ. Thienyl and phenyl alpha-halomethyl ketones: new inhibitors of glycogen synthase kinase (GSK-3beta) from a library of compound searching. *J Med Chem*. 2003; 46:4631–4633. [PubMed: 14561081]
14. Corbit KC, Aanstad P, Singla V, Norman AR, Stainier DY, Reiter JF. Vertebrate Smoothed functions at the primary cilium. *Nature*. 2005; 437:1018–1021. [PubMed: 16136078]
15. Dave RH, Saengsawang W, Yu JZ, Donati R, Rasenick MM. Heterotrimeric G-proteins interact directly with cytoskeletal components to modify microtubule-dependent cellular processes. *Neurosignals*. 2009; 17:100–108. [PubMed: 19212143]

16. De SP, Li X, Jope RS. Regulation of Akt and glycogen synthase kinase-3 beta phosphorylation by sodium valproate and lithium. *Neuropharmacology*. 2002; 43:1158–1164. [PubMed: 12504922]
17. Dousa T, Hechter O. Lithium and brain adenylyl cyclase. *Lancet*. 1970; 1:834–835.
18. Ebstein RP, Hermoni M, Belmaker RH. The effect of lithium on noradrenaline-induced cyclic AMP accumulation in rat brain: inhibition after chronic treatment and absence of supersensitivity. *J Pharmacol Exp Ther*. 1980; 213:161–167. [PubMed: 6244392]
19. Eckly-Michel AE, Le Bec A, Lugnier C. Chelerythrine, a protein kinase C inhibitor, interacts with cyclic nucleotide phosphodiesterases. *Eur J Pharmacol*. 1997; 324:85–88. [PubMed: 9137917]
20. Eley L, Yates LM, Goodship JA. Cilia and disease. *Curr Opin Genet Dev*. 2005; 15:308–314. [PubMed: 15917207]
21. Fan S, Hurd TW, Liu CJ, Straight SW, Weimbs T, Hurd EA, Domino SE, Margolis B. Polarity proteins control ciliogenesis via kinesin motor interactions. *Curr Biol*. 2004; 14:1451–1461. [PubMed: 15324661]
22. Fitzgerald C, Sikora C, Lawson V, Dong K, Cheng M, Oko R, van der Hoorn FA. Mammalian transcription in support of hybrid mRNA and protein synthesis in testis and lung. *J Biol Chem*. 2006; 281:38172–38180. [PubMed: 17040916]
23. Frame S, Cohen P. GSK3 takes centre stage more than 20 years after its discovery. *Biochem J*. 2001; 359:1–16. [PubMed: 11563964]
24. Friedman E, Wang HY. Receptor-mediated activation of G proteins is increased in postmortem brains of bipolar affective disorder subjects. *J Neurochem*. 1996; 67:1145–1152. [PubMed: 8752121]
25. Graabaek GM. Characteristics of the two types of synoviocytes in rat synovial membrane. An ultrastructural study. *Lab Invest*. 1984; 50:690–702. [PubMed: 6727301]
26. Hall AC, Brennan A, Goold RG, Cleverley K, Lucas FR, Gordon-Weeks PR, Salinas PC. Valproate regulates GSK-3-mediated axonal remodeling and synapsin I clustering in developing neurons. *Mol Cell Neurosci*. 2002; 20:257–270. [PubMed: 12093158]
27. Hallcher LM, Sherman WR. The effects of lithium ion and other agents on the activity of myo-inositol-1-phosphatase from bovine brain. *J Biol Chem*. 1980; 255:10896–10901. [PubMed: 6253491]
28. Handel M, Schulz S, Stanarius A, Schreff M, Erdtmann-Vourliotis M, Schmidt H, Wolf G, Holtt V. Selective targeting of somatostatin receptor 3 to neuronal cilia. *Neuroscience*. 1999; 89:909–926. [PubMed: 10199624]
29. Harwood AJ. Lithium and bipolar mood disorder: the inositol-depletion hypothesis revisited. *Mol Psychiatry*. 2005; 10:117–126. [PubMed: 15558078]
30. Herbert JM, Augereau JM, Gleye J, Maffrand JP. Chelerythrine is a potent and specific inhibitor of protein kinase C. *Biochem Biophys Res Commun*. 1990; 172:993–999. [PubMed: 2244923]
31. Hiruma H, Maruyama H, Katakura T, Simada ZB, Nishida S, Hoka S, Takenaka T, Kawakami T. Axonal transport is inhibited by a protein kinase C inhibitor in cultured isolated mouse dorsal root ganglion cells. *Brain Res*. 1999; 826:135–138. [PubMed: 10216205]
32. Ho PT, Tucker RW. Centriole ciliation and cell cycle variability during G1 phase of BALB/c 3T3 cells. *J Cell Physiol*. 1989; 139:398–406. [PubMed: 2654143]
33. Huang BQ, Masyuk TV, Muff MA, Tietz PS, Masyuk AI, Larusso NF. Isolation and characterization of cholangiocyte primary cilia. *Am J Physiol Gastrointest Liver Physiol*. 2006; 291:G500–G509. [PubMed: 16899714]
34. Huangfu D, Anderson KV. Cilia and Hedgehog responsiveness in the mouse. *Proc Natl Acad Sci USA*. 2005; 102:11325–11330. [PubMed: 16061793]
35. Inhorn RC, Majerus PW. Properties of inositol polyphosphate 1-phosphatase. *J Biol Chem*. 1988; 263:14559–14565. [PubMed: 2844776]
36. Iwanaga T, Shikichi M, Kitamura H, Yanase H, Nozawa-Inoue K. Morphology and functional roles of synoviocytes in the joint. *Arch Histol Cytol*. 2000; 63:17–31. [PubMed: 10770586]
37. Izaki T, Kamakura S, Kohjima M, Sumimoto H. Phosphorylation-dependent binding of 14–3–3 to Par3beta, a human Par3-related cell polarity protein. *Biochem Biophys Res Commun*. 2005; 329:211–218. [PubMed: 15721295]

38. Koh SH, Lee YB, Kim KS, Kim HJ, Kim M, Lee YJ, Kim J, Lee KW, Kim SH. Role of GSK-3beta activity in motor neuronal cell death induced by G93A or A4V mutant hSOD1 gene. *Eur J Neurosci.* 2005; 22:301–309. [PubMed: 16045483]
39. Kuchka MR, Jarvik JW. Short-Flagella Mutants of *Chlamydomonas reinhardtii*. *Genetics.* 1987; 115:685–691. [PubMed: 17246376]
40. Leitges M, Sanz L, Martin P, Duran A, Braun U, Garcia JF, Camacho F, Diaz-Meco MT, Rennert PD, Moscat J. Targeted disruption of the zetaPKC gene results in the impairment of the NF-kappaB pathway. *Mol Cell.* 2001; 8:771–780. [PubMed: 11684013]
41. Linder JU, Schultz JE. The class III adenylyl cyclases: multi-purpose signalling modules. *Cell Signal.* 2003; 15:1081–1089. [PubMed: 14575863]
42. Manji HK, Chen G. PKC, MAP kinases and the bcl-2 family of proteins as long-term targets for mood stabilizers. *Mol Psychiatry.* 2002; 7(Suppl 1):S46–S56. [PubMed: 11986995]
43. Manji HK, Chen G, Shimon H, Hsiao JK, Potter WZ, Belmaker RH. Guanine nucleotide-binding proteins in bipolar affective disorder. Effects of long-term lithium treatment. *Arch Gen Psychiatry.* 1995; 52:135–144. [PubMed: 7848049]
44. Mann L, Heldman E, Shaltiel G, Belmaker RH, Agam G. Lithium preferentially inhibits adenylyl cyclase V and VII isoforms. *Int J Neuropsychopharmacol.* 2008; 11:533–539. [PubMed: 18205980]
45. Marmol F, Carbonell L, Cuffi ML, Forn J. Demonstration of inhibition of cyclic AMP accumulation in brain by very low concentrations of lithium in the presence of alpha-adrenoceptor blockade. *Eur J Pharmacol.* 1992; 226:93–96. [PubMed: 1356811]
46. Marshall WF, Rosenbaum JL. Intraflagellar transport balances continuous turnover of outer doublet microtubules: implications for flagellar length control. *J Cell Biol.* 2001; 155:405–414. [PubMed: 11684707]
47. Masyuk AI, Masyuk TV, Splinter PL, Huang BQ, Stroope AJ, Larusso NF. Cholangiocyte cilia detect changes in luminal fluid flow and transmit them into intracellular Ca²⁺ and cAMP signaling. *Gastroenterology.* 2006; 131:911–920. [PubMed: 16952559]
48. McGlashan SR, Cluett EC, Jensen CG, Poole CA. Primary cilia in osteoarthritic chondrocytes: from chondrons to clusters. *Dev Dyn.* 2008; 237:2013–2020. [PubMed: 18330928]
49. McGlashan SR, Jensen CG, Poole CA. Localization of extracellular matrix receptors on the chondrocyte primary cilium. *J Histochem Cytochem.* 2006; 54:1005–1014. [PubMed: 16651393]
50. Moens W, Vokaer A, Kram R. Cyclic AMP and cyclic GMP concentrations in serum- and density-restricted fibroblast cultures. *Proc Natl Acad Sci USA.* 1975; 72:1063–1067. [PubMed: 165482]
51. Montezinho LP, Mork A, Duarte CB, Penschuck S, Geraldine CF, Castro MM. Effects of mood stabilizers on the inhibition of adenylyl cyclase via dopamine D(2)-like receptors. *Bipolar Disord.* 2007; 9:290–297. [PubMed: 17430304]
52. Mori S, Tardito D, Dorigo A, Zanardi R, Smeraldi E, Racagni G, Perez J. Effects of lithium on cAMP-dependent protein kinase in rat brain. *Neuropsychopharmacology.* 1998; 19:233–240. [PubMed: 9653711]
53. Mori S, Zanardi R, Popoli M, Smeraldi E, Racagni G, Perez J. Inhibitory effect of lithium on cAMP dependent phosphorylation system. *Life Sci.* 1996; 59:L99–104.
54. Mork A, Geisler A. The effects of lithium in vitro and ex vivo on adenylyl cyclase in brain are exerted by distinct mechanisms. *Neuropharmacology.* 1989; 28:307–311. [PubMed: 2542834]
55. Naerum L, Norkov-Lauritsen L, Olesen PH. Scaffold hopping and optimization towards libraries of glycogen synthase kinase-3 inhibitors. *Bioorg Med Chem Lett.* 2002; 12:1525–1528. [PubMed: 12031334]
56. Nakamura S, Takino H, Kojima MK. Effect of lithium on flagellar length in *Chlamydomonas reinhardtii*. *Cell Struct Funct.* 1987; 12:369–374.
57. Newman ME, Belmaker RH. Effects of lithium in vitro and ex vivo on components of the adenylyl cyclase system in membranes from the cerebral cortex of the rat. *Neuropharmacology.* 1987; 26:211–217. [PubMed: 3035412]
58. Nonaka S, Tanaka Y, Okada Y, Takeda S, Harada A, Kanai Y, Kido M, Hirokawa N. Randomization of left-right asymmetry due to loss of nodal cilia generating leftward flow of

- extraembryonic fluid in mice lacking KIF3B motor protein. *Cell*. 1998; 95:829–837. [PubMed: 9865700]
59. O'Neill DJ, Shen L, Prouty C, Conway BR, Westover L, Xu JZ, Zhang HC, Maryanoff BE, Murray WV, Demarest KT, Kuo GH. Design, synthesis, and biological evaluation of novel 7-azaindoyl-heteroaryl-maleimides as potent and selective glycogen synthase kinase-3beta (GSK-3beta) inhibitors. *Bioorg Med Chem*. 2004; 12:3167–3185. [PubMed: 15158785]
60. Oey J, Vogel A, Pollack R. Intracellular cyclic AMP concentration responds specifically to growth regulation by serum. *Proc Natl Acad Sci USA*. 1974; 71:694–698. [PubMed: 4362627]
61. Okuda H, Hirai S, Takaki Y, Kamada M, Baba M, Sakai N, Kishida T, Kaneko S, Yao M, Ohno S, Shuin T. Direct interaction of the beta-domain of VHL tumor suppressor protein with the regulatory domain of atypical PKC isoforms. *Biochem Biophys Res Commun*. 1999; 263:491–497. [PubMed: 10491320]
62. Ou Y, Rattner JB. A subset of centrosomal proteins are arranged in a tubular conformation that is reproduced during centrosome duplication. *Cell Motil Cytoskeleton*. 2000; 47:13–24. [PubMed: 11002307]
63. Ou YY, Mack GJ, Zhang M, Rattner JB. CEP110 and ninein are located in a specific domain of the centrosome associated with centrosome maturation. *J Cell Sci*. 2002; 115:1825–1835. [PubMed: 11956314]
64. Ou YY, Zhang M, Chi S, Matyas JR, Rattner JB. Higher order structure of the PCM adjacent to the centriole. *Cell Motil Cytoskeleton*. 2003; 55:125–133. [PubMed: 12740873]
65. Pasquale SM, Goodenough UW. Cyclic AMP functions as a primary sexual signal in gametes of *Chlamydomonas reinhardtii*. *J Cell Biol*. 1987; 105:2279–2292. [PubMed: 2824527]
66. Pazour GJ, Dickert BL, Vucica Y, Seeley ES, Rosenbaum JL, Witman GB, Cole DG. *Chlamydomonas* IFT88 and its mouse homologue, polycystic kidney disease gene *tg737*, are required for assembly of cilia and flagella. *J Cell Biol*. 2000; 151:709–718. [PubMed: 11062270]
67. Pazour GJ, Rosenbaum JL. Intraflagellar transport and cilia-dependent diseases. *Trends Cell Biol*. 2002; 12:551–555. [PubMed: 12495842]
68. Pazour GJ, San Agustin JT, Follit JA, Rosenbaum JL, Witman GB. Polycystin-2 localizes to kidney cilia and the ciliary level is elevated in orpk mice with polycystic kidney disease. *Curr Biol*. 2002; 12:R378–R380. [PubMed: 12062067]
69. Pedersen LB, Veland IR, Schroder JM, Christensen ST. Assembly of primary cilia. *Dev Dyn*. 2008; 237:1993–2006. [PubMed: 18393310]
70. Phiel CJ, Klein PS. Molecular targets of lithium action. *Annu Rev Pharmacol Toxicol*. 2001; 41:789–813. [PubMed: 11264477]
71. Quiroz JA, Gould TD, Manji HK. Molecular effects of lithium. *Mol Interv*. 2004; 4:259–272. [PubMed: 15471909]
72. Quiroz JA, Gould TD, Manji HK. Molecular effects of lithium. *Mol Interv*. 2004; 4:259–272. [PubMed: 15471909]
73. Raychowdhury MK, Ramos AJ, Zhang P, McLaughlin M, Dai XQ, Chen XZ, Montalbetti N, Cantero MD, Ausiello DA, Cantiello HF. Vasopressin Receptor-Mediated Functional Signaling Pathway in Primary Cilia of Renal Epithelial Cells. *Am J Physiol Renal Physiol*. 2008
74. Resnick A, Hopfer U. Force-response considerations in ciliary mechanosensation. *Biophys J*. 2007; 93:1380–1390. [PubMed: 17526573]
75. Rieder CL, Jensen CG, Jensen LC. The resorption of primary cilia during mitosis in a vertebrate (PtK1) cell line. *J Ultrastruct Res*. 1979; 68:173–185. [PubMed: 480410]
76. Risby ED, Hsiao JK, Manji HK, Bitran J, Moses F, Zhou DF, Potter WZ. The mechanisms of action of lithium. II. Effects on adenylate cyclase activity and beta-adrenergic receptor binding in normal subjects. *Arch Gen Psychiatry*. 1991; 48:513–524. [PubMed: 1645514]
77. Rohatgi R, Milenkovic L, Scott MP. Patched1 regulates hedgehog signaling at the primary cilium. *Science*. 2007; 317:372–376. [PubMed: 17641202]
78. Rosenbaum JL, Moulder JE, Ringo DL. Flagellar elongation and shortening in *Chlamydomonas*. The use of cycloheximide and colchicine to study the synthesis and assembly of flagellar proteins. *J Cell Biol*. 1969; 41:600–619. [PubMed: 5783876]

79. Satir P, Christensen ST. Overview of structure and function of mammalian cilia. *Annu Rev Physiol.* 2007; 69:377–400. [PubMed: 17009929]
80. Schermer B, Ghenoiu C, Bartram M, Muller RU, Kotsis F, Hohne M, Kuhn W, Rapka M, Nitschke R, Zentgraf H, Fliegau M, Omran H, Walz G, Benzing T. The von Hippel-Lindau tumor suppressor protein controls ciliogenesis by orienting microtubule growth. *J Cell Biol.* 2006; 175:547–554. [PubMed: 17101696]
81. Schneider L, Clement CA, Teilmann SC, Pazour GJ, Hoffmann EK, Satir P, Christensen ST. PDGFR α signaling is regulated through the primary cilium in fibroblasts. *Curr Biol.* 2005; 15:1861–1866. [PubMed: 16243034]
82. Schumacher HR Jr. Ultrastructure of the synovial membrane. *Ann Clin Lab Sci.* 1975; 5:489–498. [PubMed: 812419]
83. Schwartz EA, Leonard ML, Bizios R, Bowser SS. Analysis and modeling of the primary cilium bending response to fluid shear. *Am J Physiol.* 1997; 272:F132–F138. [PubMed: 9039059]
84. Seng S, Avraham HK, Jiang S, Venkatesh S, Avraham S. KLHL1/MRP2 mediates neurite outgrowth in a glycogen synthase kinase 3 β -dependent manner. *Mol Cell Biol.* 2006; 26:8371–8384. [PubMed: 16982692]
85. Sfakianos J, Togawa A, Maday S, Hull M, Pypaert M, Cantley L, Toomre D, Mellman I. Par3 functions in the biogenesis of the primary cilium in polarized epithelial cells. *J Cell Biol.* 2007; 179:1133–1140. [PubMed: 18070914]
86. Shikichi M, Kitamura HP, Yanase H, Konno A, Takahashi-Iwanaga H, Iwanaga T. Three-dimensional ultrastructure of synoviocytes in the horse joint as revealed by the scanning electron microscope. *Arch Histol Cytol.* 1999; 62:219–229. [PubMed: 10495876]
87. Smith LA, Bukanov NO, Husson H, Russo RJ, Barry TC, Taylor AL, Beier DR, Ibraghimov-Beskrovnaia O. Development of polycystic kidney disease in juvenile cystic kidney mice: insights into pathogenesis, ciliary abnormalities, and common features with human disease. *J Am Soc Nephrol.* 2006; 17:2821–2831. [PubMed: 16928806]
88. Solter KM, Gibor A. Removal and recovery of mating receptors on flagella of *Chlamydomonas reinhardtii*. *Exp Cell Res.* 1978; 115:175–181. [PubMed: 680009]
89. Somlo S, Ehrlich B. Human disease: calcium signaling in polycystic kidney disease. *Curr Biol.* 2001; 11:R356–R360. [PubMed: 11369247]
90. Tam LW, Lefebvre PA. Cloning of flagellar genes in *Chlamydomonas reinhardtii* by DNA insertional mutagenesis. *Genetics.* 1993; 135:375–384. [PubMed: 8244002]
91. Thoma CR, Frew IJ, Hoerner CR, Montani M, Moch H, Krek W. pVHL and GSK3 β are components of a primary cilium-maintenance signalling network. *Nat Cell Biol.* 2007; 9:588–595. [PubMed: 17450132]
92. Tuxhorn J, Daise T, Dentler WL. Regulation of flagellar length in *Chlamydomonas*. *Cell Motil Cytoskeleton.* 1998; 40:133–146. [PubMed: 9634211]
93. Verghese E, Weidenfeld R, Bertram JF, Ricardo SD, Deane JA. Renal cilia display length alterations following tubular injury and are present early in epithelial repair. *Nephrol Dial Transplant.* 2008; 23:834–841. [PubMed: 17962379]
94. Wang L, Weidenfeld R, Verghese E, Ricardo SD, Deane JA. Alterations in renal cilium length during transient complete ureteral obstruction in the mouse. *J Anat.* 2008; 213:79–85. [PubMed: 18537851]
95. Wasserman MJ, Corson TW, Sibony D, Cooke RG, Parikh SV, Pennefather PS, Li PP, Warsh JJ. Chronic lithium treatment attenuates intracellular calcium mobilization. *Neuropsychopharmacology.* 2004; 29:759–769. [PubMed: 14970832]
96. Wheatley DN, Bowser SS. Length control of primary cilia: analysis of monociliate and multiciliate PtK1 cells. *Biol Cell.* 2000; 92:573–582. [PubMed: 11374436]
97. Wikramanayake AH, Brandhorst BP, Klein WH. Autonomous and non-autonomous differentiation of ectoderm in different sea urchin species. *Development.* 1995; 121:1497–1505. [PubMed: 7789279]
98. Wilson NF, Lefebvre PA. Regulation of flagellar assembly by glycogen synthase kinase 3 in *Chlamydomonas reinhardtii*. *Eukaryot Cell.* 2004; 3:1307–1319. [PubMed: 15470259]

99. WYLLIE JC, MORE RH, Haust MD. THE FINE STRUCTURE OF NORMAL GUINEA PIG SYNOVIUM. *Lab Invest.* 1964; 13:1254–1263. [PubMed: 14212357]
100. Yoder BK, Hou X, Guay-Woodford LM. The polycystic kidney disease proteins, polycystin-1, polycystin-2, polaris, and cystin, are co-localized in renal cilia. *J Am Soc Nephrol.* 2002; 13:2508–2516. [PubMed: 12239239]
101. Young LT, Li PP, Kish SJ, Siu KP, Kamble A, Hornykiewicz O, Warsh JJ. Cerebral cortex Gs alpha protein levels and forskolin-stimulated cyclic AMP formation are increased in bipolar affective disorder. *J Neurochem.* 1993; 61:890–898. [PubMed: 8395565]
102. Young LT, Li PP, Kish SJ, Siu KP, Warsh JJ. Postmortem cerebral cortex Gs alpha-subunit levels are elevated in bipolar affective disorder. *Brain Res.* 1991; 553:323–326. [PubMed: 1933291]

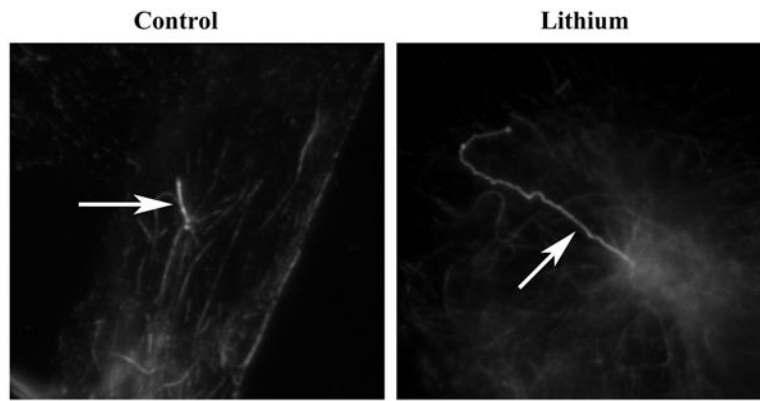


Figure 1. Lithium induces primary cilia elongation in serum-starved FLS cells

Serum-starved cells were treated with 100 mM lithium chloride for 12 hrs, fixed with cold methanol, stained with anti-acetylated tubulin antibody, and examined by indirect immunofluorescence microscopy. Primary cilium elongation is seen in serum-starved FLS cells after lithium treatment. Control: untreated sample; Lithium: lithium-treated cells. Arrows denote the primary cilia.

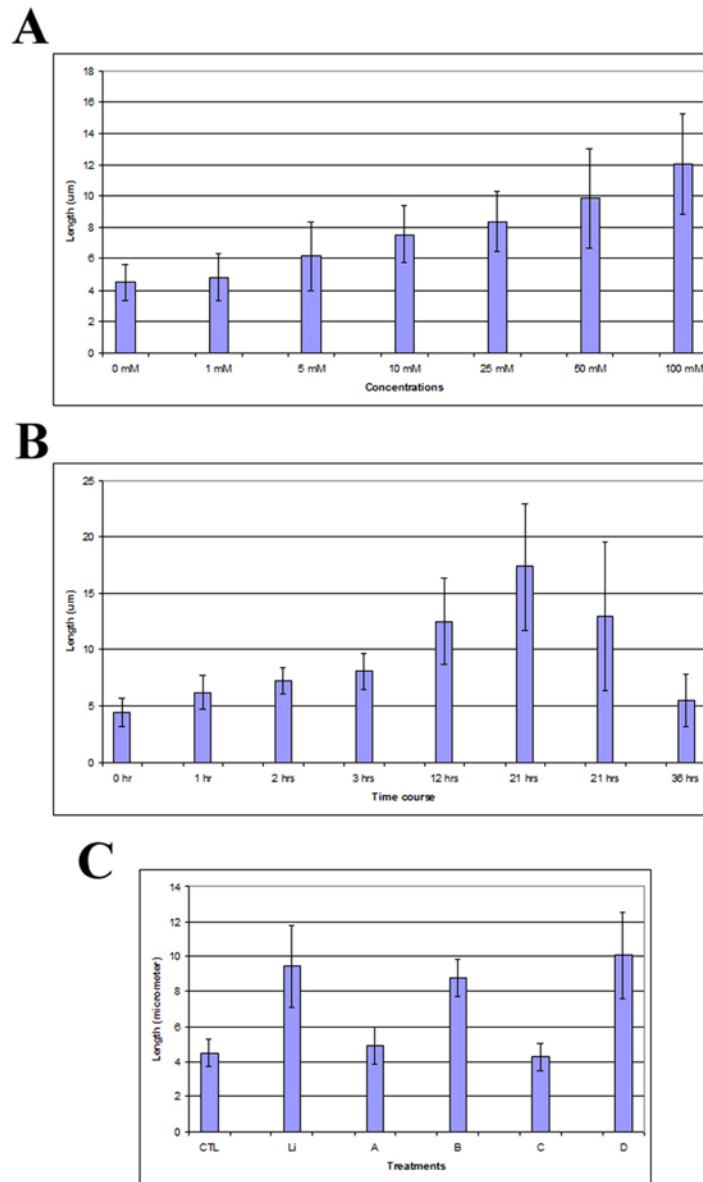


Figure 2. Dynamics of primary cilium elongation after lithium treatment

FLS cells were serum-starved for 48 hrs, and then were treated with lithium at various times and concentrations as indicated. Cells were fixed in cold methanol, stained with anti-acetylated tubulin antibody, and examined by indirect immunofluorescence microscopy. The lengths of primary cilia were measured as indicated in Materials and Methods. Panel A, dose-response of primary cilia length after lithium treatment for 12 hrs. Panel B, Time course of primary cilia length after lithium treatment at 100 mM concentration. Panel C, Protein synthesis inhibition and primary cilium elongation. Serum-starved FLS cells were treated as follows: CTL, primary cilia in untreated control cells. Cells were first incubated with serum-free medium for 3 hrs, followed by an additional 7 hrs fresh serum-free medium incubation. Li, lithium-treated cells. Cells were first incubated with serum-free medium for 3 hrs, followed by 100 mM lithium treatment for 7 hrs in serum-free medium. A–D, cells were

treated with 50 $\mu\text{g/ml}$ (A and B) or 250 $\mu\text{g/ml}$ (C and D) of cycloheximide. A, 50 $\mu\text{g/ml}$ cycloheximide for 10 hrs; B, 50 $\mu\text{g/ml}$ cycloheximide for 3 hrs followed by co-treatment with 100 mM lithium/50 $\mu\text{g/ml}$ cycloheximide for 7 hrs; C, 250 $\mu\text{g/ml}$ cycloheximide for 10 hrs; D, 250 $\mu\text{g/ml}$ cycloheximide for 3 hrs followed by co-treatment with 100 mM lithium/250 $\mu\text{g/ml}$ cycloheximide for 7 hrs. Error bars indicate standard deviation.

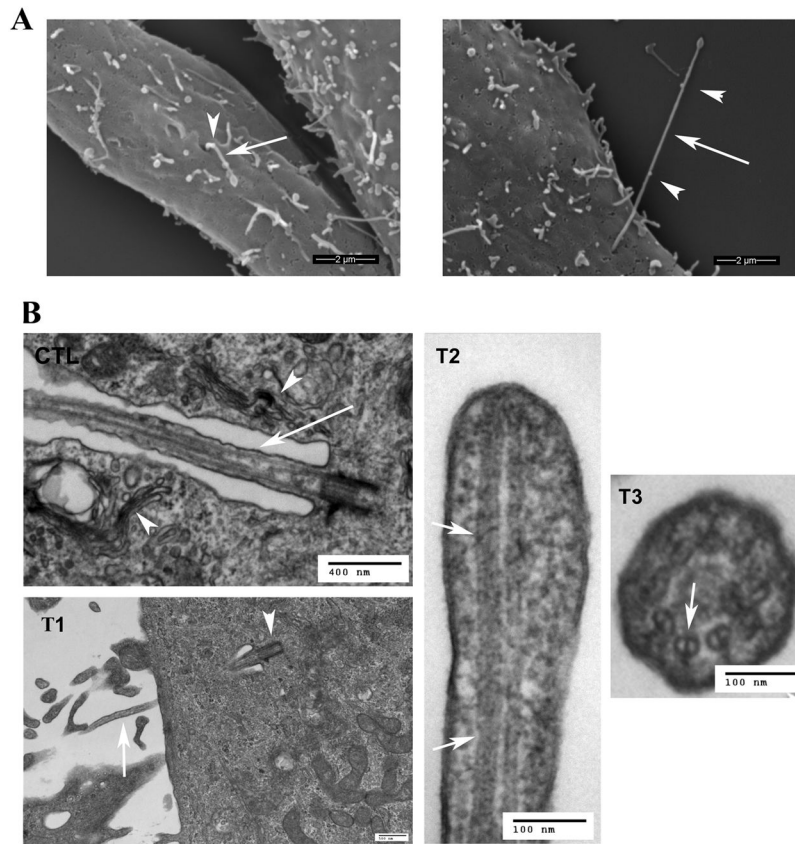


Figure 3. Ultrastructural analysis of primary cilia

A. Scanning electron microscopy. Left image, untreated FLS cells; Right image, lithium-treated FLS cells. FLS cells were treated with 100 mM lithium chloride for 12 hrs. Shown are the extracellular portion of the primary cilia (arrows) and potential IFT particles (arrowheads). Bar = 2 μ m. **B.** Transmission electron microscopy. CTL, untreated control sample. The arrow points to the portion of a primary cilium that lies in an invagination of the plasma membrane. Note that the invagination is lined with Golgi complexes (arrowheads). T1–T3, serum-starved FLS cells treated with 100 mM lithium chloride for 12 hrs. T1, an elongated primary cilium extending from the basal body (arrowhead) into the invagination of the plasma membrane and protruding outside the cell (arrow). T2, longitudinal section of the tip of a primary cilium. T3, cross-section of an elongated primary cilium inside the invagination of the plasma membrane. Note that both longitudinal (T2, arrows) and cross-sections (T3, arrow) reveal double microtubules, and that these doublets extend to the tip of the cilium (T2). Bars in different images represent different length. CTL, bar = 400 nm; T1, bar = 500 nm; T2, bar = 100 nm. T3, bar = 100 nm.

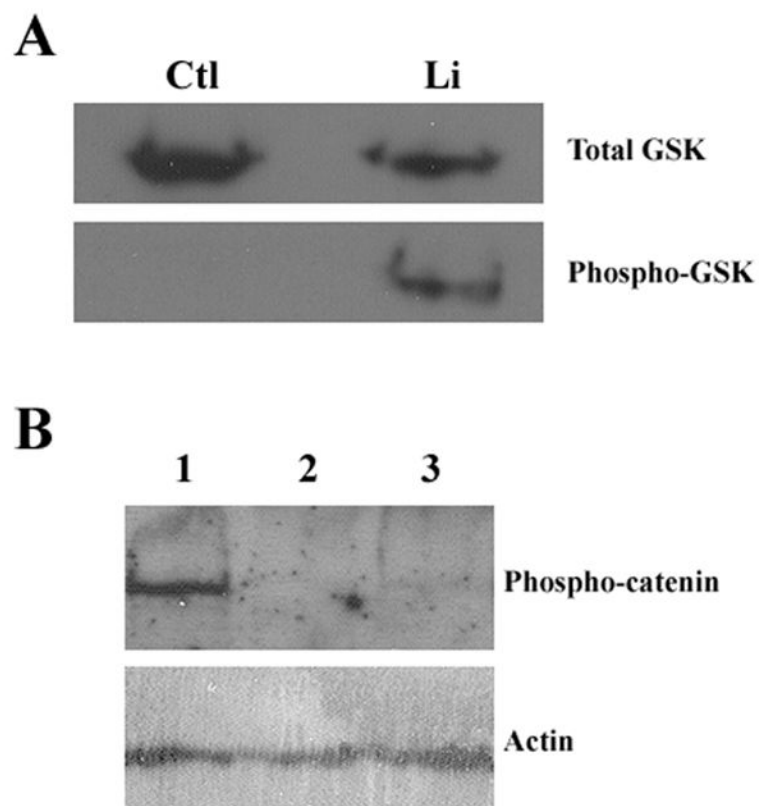


Figure 4. Protein phosphorylation or dephosphorylation after lithium treatment

FLS cells were serum-starved for 48 hrs and then were treated with 100 mM lithium chloride for 12 hrs. Cells were collected, and proteins were fractionated by SDS-PAGE. A, Western blot analysis of GSK-3 β . Upper panel, total GSK-3 β as revealed by using an antibody raised against unphosphorylated protein. Lower panel, phosphorylated GSK-3 β as revealed by using an antibody specific for the phospho-serine (Ser-9) epitope of the protein. Ctl, control cells treated with fresh serum-free medium; Li, cells treated with lithium. B, Western blot analysis of β -catenin. Upper panel, phosphorylated β -catenin detected using an antibody specific for phosphorylated (Thr-41/Ser-37/Ser-33) β -catenin protein. Lower panel, actin proteins detected using anti- β -actin antibody, indicating protein loading. Lane 1, cells treated with fresh serum-free medium; Lane 2, cells treated with lithium; Lane 3, cells treated with GSK-3 β inhibitor VII.

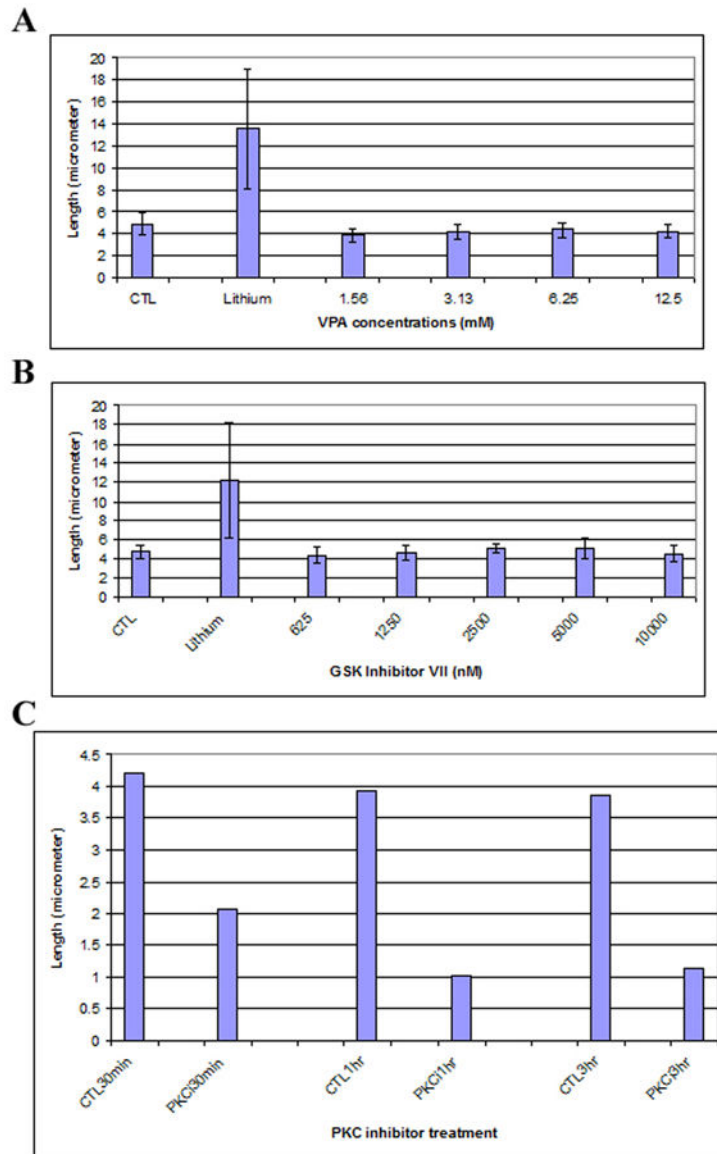


Figure 5. Protein kinases and primary cilia elongation

FLS cells were serum-starved for 48 hrs and then were treated with different drugs for various times. **A**, Serum-starved FLS cells were treated with valproate for 12 hrs at the indicated concentrations. The graphs show average length of 150 primary cilia from three independent experiments, with error bars showing standard deviation. CTL, control cells were treated with fresh serum-free medium; Lithium, cells were treated with 100 mM lithium; 1.56 mM-12.5, valproate concentrations (mM). **B**. Serum-starved FLS cells were treated with GSK-3 inhibitor VII for 12 hrs at the indicated concentrations. Shown is the average length of 150 primary cilia from three independent experiments, with error bars showing standard deviation. CTL, control cells treated with fresh serum-free medium; Lithium, cells treated with 100 mM lithium; 625–10000, GSK inhibitor VII concentrations (nM). **C**. Effect of protein kinase C inhibitor on primary cilia. Serum-starved FLS cells were treated with 10 μ M PKC protein kinase inhibitor for 30 min, 1 hr and 3 hrs, respectively.

Shown are average lengths of 150 primary cilia from three independent experiments with error bars showing standard deviation. CTL30min, CTL1hr, CTL3hr; control cells treated with fresh serum-free medium for 30 min, 1 hr and 3 hrs, respectively. PKCi30min, PKC1hr, PKCi3hr: cells treated with 10 μ M PKC inhibitor for 30 min, 1 hr, and 3 hrs, respectively.

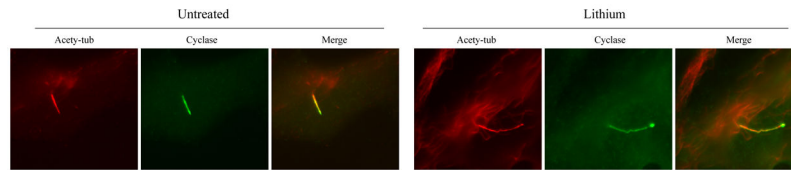


Figure 6. Adenylate cyclase III and primary cilia

Adenylate cyclase III is present at primary cilia of FLS cells. Serum-starved FLS cells were treated with lithium, fixed in cold methanol, and stained with antibodies to acetylated tubulin and adenylate cyclase III. Untreated, cells treated with fresh serum-free medium; Lithium, cells treated with 50 mM lithium for 12 hrs. Acety-tub, staining with anti-acetylated tubulin antibody; Cyclase, cells staining with anti-adenylate cyclase III antibody; Merge, composite of both images.

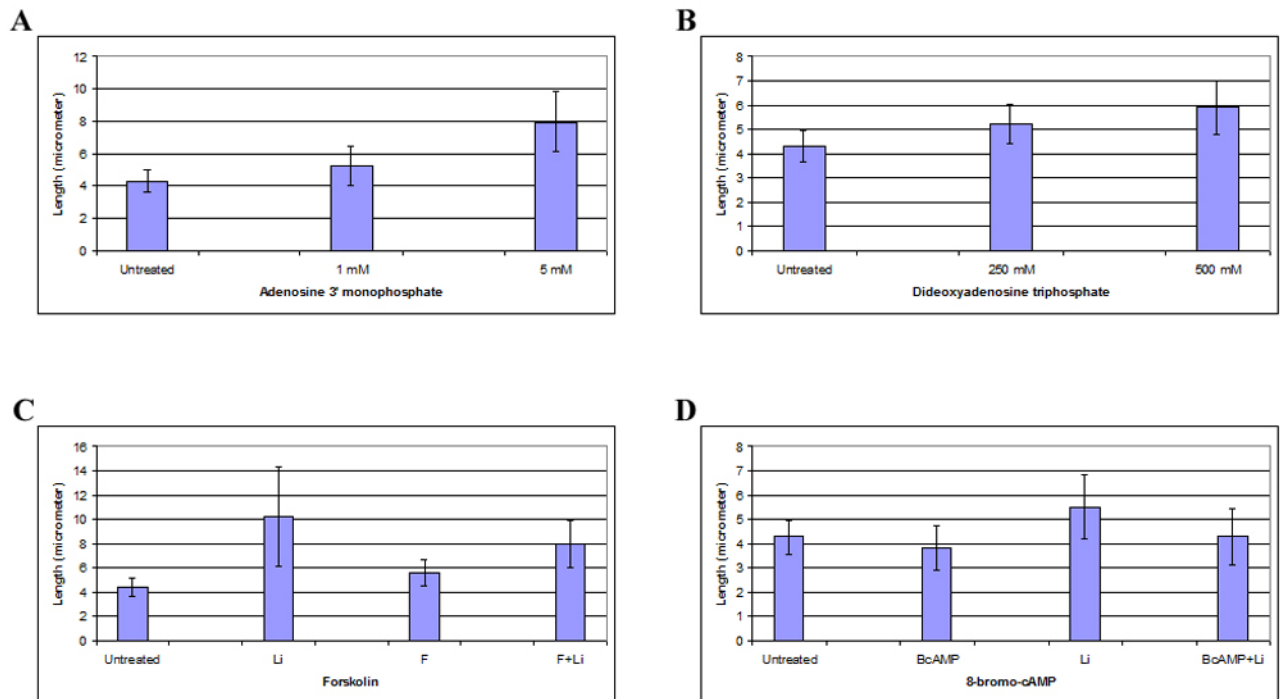


Figure 7. Adenylate cyclase III activity and primary cilia elongation

FLS cells were serum-starved for 48 hrs and then were treated with P-site inhibitors or activators. **A**, Cells were treated with adenosine 3' monophosphate (3'-AMP) for 60 hrs. Shown are average lengths of 150 primary cilia obtained from three independent experiments, with error bars indicating standard deviation. Untreated, control cells receiving fresh serum-free medium; 1 mM and 5 mM, 3'-AMP concentrations. **B**, Serum-starved cells were treated with P-site inhibitor dideoxyadenosine triphosphates (DDAT) for 60 hrs. Shown are average lengths of 150 primary cilia from three independent experiments. Untreated, cells treated with fresh serum-free medium; 250 mM and 500 mM, DDAT concentrations. **C**, forskolin interference. Shown are average lengths of 150 primary cilia obtained from three independent experiments. Untreated, serum-starved cells incubated with fresh serum-free medium for 7 hrs; Li, cells treated with 50 mM lithium for 7 hrs; F, cells incubated with 0.5 mM forskolin for 7 hrs; F+L, cells first incubated with 0.5 mM forskolin for 2 hrs and then treated with 50 mM lithium for 7 hrs. **D**, 8-bromo-cAMP interference. Shown are average lengths of 150 primary cilia obtained from three independent experiments. Untreated, serum-starved cells incubated with fresh serum-free medium for 5 hrs; Li, cells treated with 25 mM lithium for 5 hrs; BcAMP, cells incubated with 100 μ M 8-bromo-cAMP for 5 hrs; BcAMP+Li, cells first incubated with 100 μ M 8-bromo-cAMP for 1 hr and then treated with 25 mM lithium for 5 hrs.

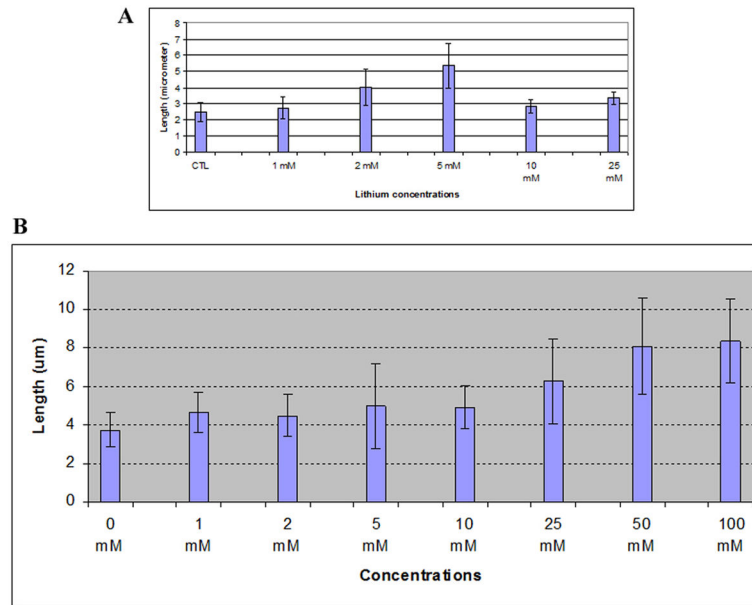


Figure 8. Dose response for lithium in two neuronal cell types
 Cells were serum-starved for 48 hrs and then were treated with lithium at the concentrations indicated in the figure. **A**, PC-12 cells; **B**, astrocytes. Shown are average lengths of 150 primary cilia obtained from three independent experiments, with error bars indicating standard deviation.

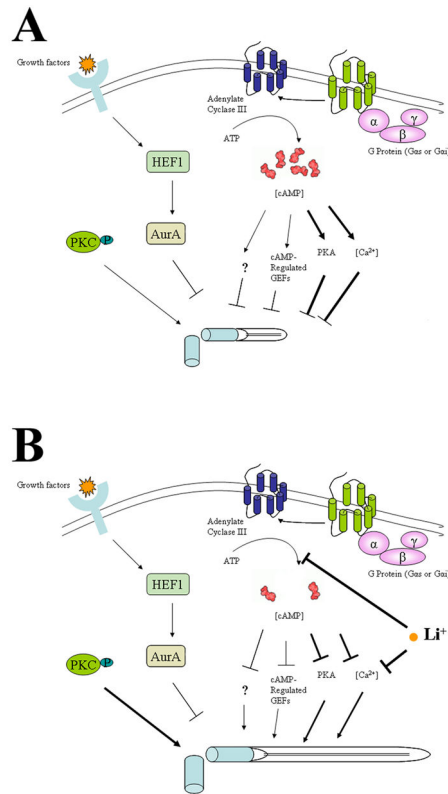


Figure 9. A model of primary cilia growth and elongation

A. Primary cilia in an untreated cell. Primary cilia start to form after mitosis. During the early stage of G1 (or experimentally in G0 cells) primary cilia start to grow. With cell cycle progression (or with time increase in the quiescent state), cAMP and calcium concentrations increase. With participation of other factors (including cAMP-responsive GTP exchange protein or unknown factors, PKC and Aurora kinase) the increased cAMP and calcium levels prevent primary cilia from further growth. At this stage, there is equilibrium between growth and regression of primary cilia, balanced by all factors. **B.** Lithium and primary cilia. Addition of lithium to the cell culture causes inhibition of adenylate cyclase III, reducing cAMP and calcium levels. Lithium may also directly attenuate the intracellular calcium concentration. As a result, lithium disturbs the balance, favoring primary cilia to resume their growth.